

Determination of dynamical quantum phase transitions for boson systems using the Loschmidt cumulants method

Pengju Zhao^{1,*}, Jingxin Sun,² Shengjie Jin,¹ Zhongshu Hu,¹ Dingping Li,¹ Xiong-Jun Liu,¹ Jörg Schmiedmayer,³ and Xuzong Chen^{4,†}

¹*School of Physics, Peking University, Beijing 100871, China*

²*Science and Technology on Metrology and Calibration Laboratory, Beijing Institute of Radio Metrology and Measurements, Beijing, 100854, China*

³*Vienna Center for Quantum Science and Technology, Atominstytut, TU-Wien, Stadionallee 2, 1020 Vienna, Austria*

⁴*School of Electronics, Peking University, Beijing 100871, China*



(Received 2 August 2023; accepted 28 November 2023; published 8 January 2024)

We study the dynamical quantum phase transition (DQPT) of the Bose-Hubbard model utilizing the recently developed Loschmidt cumulants method. We determine the complex Loschmidt zeros of the Loschmidt amplitude analogous to the Lee-Yang zeros of the thermal partition function. We obtain the DQPT critical points through identifying the crossing points with the imaginary axis. The critical points show high accuracy when compared to those obtained using the matrix product states method. In addition, we show how the critical points of DQPT can be determined by analyzing the energy fluctuation of the initial state, which makes it a valuable tool for future studies in this area. Finally, DQPT in the extended Bose-Hubbard model is also investigated.

DOI: [10.1103/PhysRevA.109.013309](https://doi.org/10.1103/PhysRevA.109.013309)

I. INTRODUCTION

Nonequilibrium dynamics has drawn much attention in recent years [1–8]. One major achievement is the investigation of dynamical quantum phase transitions (DQPTs). DQPTs concern the critical behavior of many-body systems that are driven out of equilibrium via sudden quenches. In fact, there are two types of DQPTs. The first one concerns the nonanalytical change of order parameter along the nonequilibrium evolution [8,9]. For instance, in the reference [8], it was observed that the evolution dynamics of the spin order parameter undergoes a significant change when the perturbation exceeds a certain threshold value. In this study, we specifically concentrate on the second type of DQPT that has been proposed in recent years [10,11]. This type of DQPT is inspired by the similarity between the Loschmidt amplitude

$$G(t) = \langle \psi_0 | e^{-i\hat{H}t} | \psi_0 \rangle, \quad (1)$$

where $|\psi_0\rangle$ is the ground state of the prequench Hamiltonian and the canonical partition function

$$Z(\beta) = \text{Tr} e^{-\beta\hat{H}}, \quad (2)$$

where β is the inverse temperature. When a DQPT occurs, the Loschmidt rate function

$$\lambda(t) = -\frac{1}{L} \ln |G(t)|^2 \quad (3)$$

develops nonanalytic behavior, where L is the length of the system.

It is expected to capture unique features of nonequilibrium dynamics [12–18]. Due to the absence of a direct connection to local order parameters, experimental verification of this particular type of DQPT remains challenging [19,20], particularly for systems with interaction.

The Bose-Hubbard model is a well-known model for investigating the many-body phases, with numerous studies conducted on both equilibrium and nonequilibrium phases. For nonequilibrium dynamics, the Kibble-Zurek mechanism [21–23] and DQPTs [24] have been studied for the Bose-Hubbard model. A DQPT occurs in the Bose-Hubbard model when the system is quenched from the Mott-insulator phase to the superfluid phase, as shown in Fig. 1(a). DQPT also happens in the extended Bose-Hubbard model for an interaction quench through the Mott insulator-Haldane insulator transition and the Haldane insulator-density wave transition [25].

DQPTs have been investigated by exactly solvable models [10,26,27]. Nonetheless, the dynamics of interacting quantum many-body systems remains a formidable challenge. Traditionally, real time evolution of the Loschmidt rate function is needed for determining the critical points. Usually large system size is required to precisely locate the critical times. Recently, a new method [28,29] has been proposed to determine the dynamical critical points. This method determines zeros of the dynamical Loschmidt amplitude analogous to the Lee-Yang zeros [30–32] of the thermal phase transition. The critical points are determined from the crossing points of the thermodynamics lines of zeros with the imaginary axis, as shown in Fig. 1(b). Remarkably, this method works well for spin chain with length about 10 to 20. So it is desirable for implementation of this method for boson systems. Moreover, this method offers a viable approach to determine the

*1801110090@pku.edu.cn

†xuzongchen@pku.edu.cn

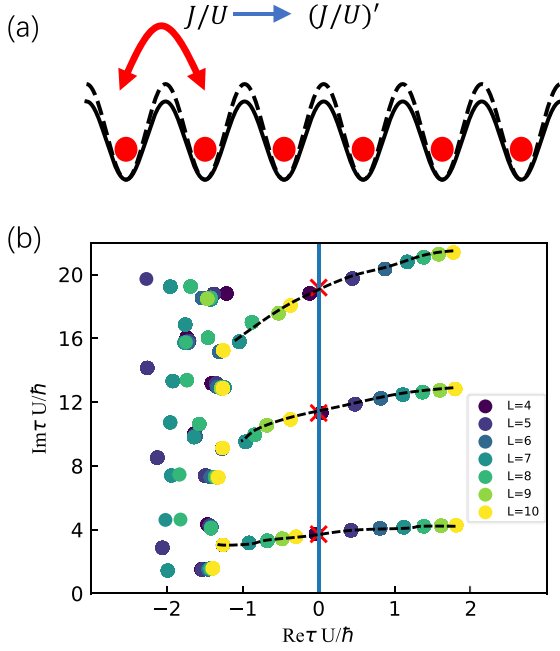


FIG. 1. Dynamical quantum phase transition. (a) A sudden quench of the hopping parameter causes a dynamical quantum phase transition in a Bose-Hubbard chain. (b) The rate function's singularities are connected to the points where the Loschmidt amplitude becomes zero within the complex-time plane. These zero points coalesce to form continuous lines in the thermodynamic limit. Identifying the critical times involves locating the intersections between these lines and the imaginary axis.

dynamical critical points by analyzing the energy fluctuations of the initial state. Implementation of this method may also provide experimental inspirations of DQPT to boson systems.

Here we focus on DQPTs in the Bose-Hubbard model following a quench. In Sec. II, we introduce the basic ideas for determining the critical points using Loschmidt cumulants, as illustrated in Ref. [28]. In Sec. III, we investigate dynamical phase transitions in the Bose-Hubbard model and accurately determine the critical points. In Sec. IV, we consider the nearest-neighbor interaction, and investigate quenches across topologically distinct phases. In Sec. V, we show that how the critical points of DQPT can be determined by analyzing the energy fluctuation of the initial state. In Sec. VI, we present our conclusions and offer an outlook on potential directions for future advancements.

II. DYNAMICAL PHASE TRANSITION AND LOSCHMIDT CUMULANTS

Here, we consider the Loschmidt amplitude on the complex time plane

$$Z(\tau) = \langle \psi_0 | e^{-\tau \hat{H}} | \psi_0 \rangle. \quad (4)$$

For a finite system, the Loschmidt amplitude is an entire function. According to the factorization theorem [33], the Loschmidt amplitude can be written as

$$Z(\tau) = e^{\alpha \tau} \prod_{k=0}^{\infty} \left(1 - \frac{\tau}{\tau_k} \right), \quad (5)$$

where α is a constant, and τ_k are complex zeros of the Loschmidt amplitude. In the thermodynamics limit, the complex zeros form lines or areas. When such a line intersects or a boundary of a region touches the imaginary axis, a DQPT takes place.

The approach which is used to determine the dynamical critical points involves obtaining the line of zeros in the thermodynamic limit. As illustrated in Ref. [28], the Loschmidt cumulants and the Loschmidt moments are used to calculate the Loschmidt zeros. They are defined as

$$\langle \langle \hat{H}^n \rangle \rangle_{\tau} = (-1)^n \partial_{\tau}^n \ln Z(\tau), \quad (6)$$

$$\langle \hat{H}^n \rangle = (-1)^n \frac{\partial_{\tau}^n Z(\tau)}{Z(\tau)} = \frac{\langle \psi_0 | \hat{H}^n e^{-\hat{H}\tau} | \psi_0 \rangle}{\langle \psi_0 | e^{-\hat{H}\tau} | \psi_0 \rangle}. \quad (7)$$

The Loschmidt cumulants can be obtained by calculating the Loschmidt moments. At $\tau = 0$, the Loschmidt moments reduce to the ordinary moments (7) of the postquench Hamiltonian with respect to the initial state as $\langle \hat{H}^n \rangle = \langle \Psi_0 | \hat{H}^n | \Psi_0 \rangle$.

On the other hand, the Loschmidt cumulants are related to the Loschmidt zeros through

$$\langle \langle \hat{H}^n \rangle \rangle_{\tau} = (-1)^{n-1} (n-1)! \sum_{k=0}^{\infty} \frac{1}{(\tau_k - \tau)^n}. \quad (8)$$

The Loschmidt cumulants are primarily influenced by the zeros that are closest to the base point τ . The contribution of each zero to the cumulants decreases rapidly with its inverse distance to the power of the cumulant order n . Thus, by computing $2m$ high-order Loschmidt cumulants, it is possible to invert Eq. (8) and then obtain the m closest zeros to the base point. Additional elaboration can be found in Appendix A of Ref. [28].

III. THE BOSE-HUBBARD MODEL

In this study, we explore DQPTs in the one-dimensional Bose-Hubbard model, characterized by the Hamiltonian:

$$\hat{H} = -J \sum_{i=1}^L (a_i^{\dagger} a_{i+1} + a_{i+1}^{\dagger} a_i) + \frac{U}{2} \sum_{i=1}^L n_i (n_i - 1) \quad (9)$$

Here a_i^{\dagger} is the creation operator for a boson on site i , a_i is the annihilation operator for a boson on site i , $n_i = a_i^{\dagger} a_i$ is the occupation operator for a boson on site i , J denotes the hopping amplitude between nearest neighbors, U denotes the onsite interaction strength. L is the length of the Bose-Hubbard chain. To minimize boundary effects, we impose the periodic boundary condition, i.e., $a_{L+1} = a_1$, $a_{L+1}^{\dagger} = a_1^{\dagger}$.

The properties of the Hamiltonian are determined by the dimensionless ratio $s = J/U$, and a phase transition occurs at the critical value of $s_c = 0.297$ for unit filling, which separates the system into a Mott-insulator phase for $s < s_c$ and a superfluid phase for $s > s_c$.

We are now prepared to study DQPTs in the Bose-Hubbard chain. We initialize the system in the superfluid ground state with a parameter value of $s_0 = 0.36$. Probability of the atom occupation number for $n_{\text{occu}} > 3$ is less than 0.03% for the initial state. The local Hilbert space is truncated to atom number occupation $n_{\text{occu}} = 3$ for balance of efficiency and accuracy.

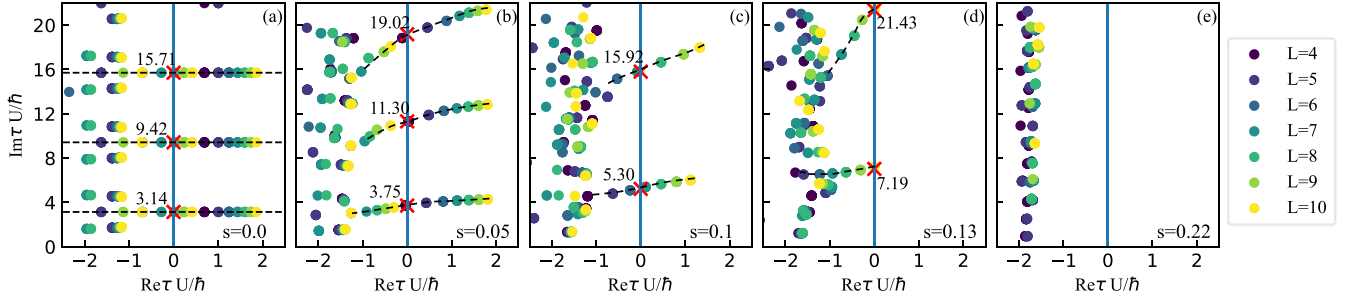


FIG. 2. Determination of critical points for the Bose-Hubbard model. Complex zeros for different system sizes ($L = 4-10$) are shown. We quench the system from the superfluid phase with initial parameter $s_0 = J/U = 0.36$ to the Mott phase. In (a), horizontal lines with $\text{Im}\tau U/\hbar = \pi, 3\pi, 5\pi$ are shown. The critical time t_c is determined as the point where the imaginary axis intersects the line connecting the zero τ_- with the smallest negative real part (in absolute value) and the zero τ_+ with the smallest positive real part. The critical time obtained using MPS method (red cross) with length of 120 sites are drawn for comparison. (b)–(e) Same as in (a) but for different parameter values: $s = 0.05$ in (b), $s = 0.1$ in (c), $s = 0.13$ in (d), and $s = 0.22$ in (e).

In our calculations, we limit the summation in Eq. (8) to the range $k = 0$ to $k = 6$. Thus, we can extract the seven zeros closest to the movable basepoint using Loschmidt cumulants of order $n = 9$ to $n = 22$. In our time evolution of the wavefunction, we select the Krylov subspace dimension to be $N_{\text{vec}} = 8$ and the time step for evolution to be $\delta\tau = 0.01$.

We perform a quench into the Mott-insulator phase with $s < 0.297$ for later times. The same quench parameters have been explored in Ref. [24] using matrix product states (MPS) method. Here we employ the MPS method for benchmark.

Figure 2 shows the complex zeros of the Loschmidt amplitude. For the $J = 0$ case, the system undergoes periodic evolution with period $T = \frac{2\pi\hbar}{U}$. The first critical time is $t_1 = \frac{\pi}{U}$. As expected, the zeros forms a line around $t = \frac{\pi\hbar}{U}, \frac{3\pi\hbar}{U}, \frac{5\pi\hbar}{U}$ on the imaginary axis and the system experiences periodic dynamics. As the tunneling amplitude is incrementally increased, it can be observed in Figs. 2(b)–2(d) that the Loschmidt zeros gradually shift the critical crossing point with the imaginary axis towards later times. Finally the thermodynamic lines of zeros no longer cross the imaginary axis and all zeros locate on the negative part of the complex plane as in Fig. 2(e). We provide an explanation in Appendix A.

The critical times obtained from the crossings of the thermodynamic lines of zeros with the imaginary axis are in excellent agreement with the critical times obtained using the MPS method. To quantify the accuracy of the Loschmidt cumulants method, we determine the critical points and compare them with those obtained using MPS method. We find that for all typical cases in Fig. 2 the discrepancy is lower than 2%. It is worth noting that these results are obtained for rather short length from $L = 4$ to $L = 10$. The use of such system sizes makes the approach very attractive for strongly interacting systems.

IV. THE EXTENDED BOSE-HUBBARD MODEL

We will now explore DQPTs in the extended Bose-Hubbard model, which includes nearest-neighbor interactions and exhibits rich phase diagrams such as the Haldane insulator and the charge density wave. The Hamiltonian for the

extended Bose-Hubbard model is given by

$$\hat{H} = -J \sum_{i=1}^L (a_i^\dagger a_{i+1} + a_{i+1}^\dagger a_i) + \frac{U}{2} \sum_{i=1}^L n_i(n_i - 1) \quad (10)$$

$$+ V \sum_{i=1}^L n_i n_{i+1}.$$

Here V denotes the nearest neighbor interaction strength. For a ratio of interaction to hopping strength of $U/J = 5$, the equilibrium phase transition point is $p = V/J = 2.95$ for the Mott insulator-Haldane insulator transition and $p = 3.53$ for the Haldane insulator-density wave transition [34]. We adopt periodic boundary conditions in this study [35,36].

We quench from the Mott phase $p_0 = 1.0$ to larger nearest neighbor interaction [25]. The results are shown in Fig. 3. From the thermodynamic line of the Loschmidt zeros, the first critical point can be identified. Dynamical quantum phase transition occurs at about $p = 3.5$. As we increase the ratio p , dynamical phase transition happens at earlier times. For typical cases in Figs. 2(c)–2(d), the discrepancy is lower than 6%. The discrepancy is larger near the equilibrium phase transition points. This may be due to the finite-size effect (see Appendix B). For further improvement, twisted boundary conditions may be introduced [28]. Although our study focuses on a narrow range of parameters, it is feasible to investigate DQPTs for other parameter ranges in the extended Bose-Hubbard model as well.

V. EXPERIMENTAL PERSPECTIVE OF THE LOSCHMIDT ZEROS

Finally, we demonstrate the ability to predict DQPT solely through measuring the energy fluctuations in the initial state. At $\tau = 0$, the Loschmidt moments transform into the regular moments (7) of the postquench Hamiltonian with respect to the initial state, as indicated by: $\langle \hat{H}^n \rangle = \langle \Psi_0 | \hat{H}^n | \Psi_0 \rangle$. If we expand the wavefunction with respect to the postquench Hamiltonian $|\Psi_0\rangle = \sum_m a_m |\tilde{\Psi}_m\rangle$, we get $\langle \hat{H}^n \rangle = \sum_m P(E_m) E_m^n$, where $P(E_m) = |a_m|^2$. Therefore, through a series of successive preparations of the system in the state $|\psi_0\rangle$ and subsequent energy measurements concerning the

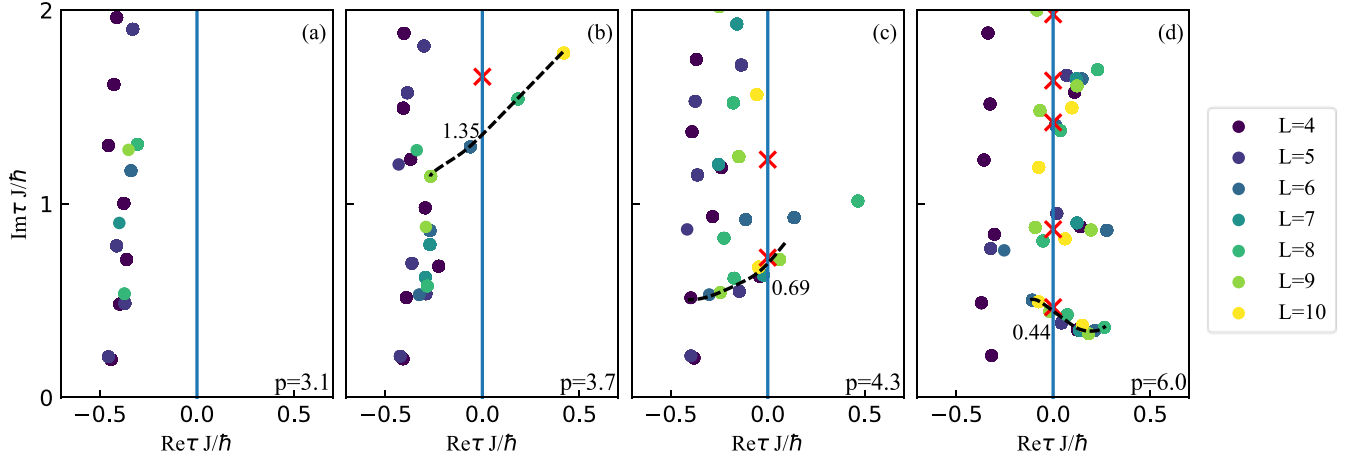


FIG. 3. Determination of critical points for the extended Bose-Hubbard model. We quench the system from the Mott insulator phase with initial parameter $U/J = 5$, $p_0 = V/J = 1.0$. We quench the system to the final Hamiltonian of various p . (a)–(d) illustrate DQPTs corresponding to various final parameters: $p = 3.1$ in (a), $p = 3.7$ in (b), $p = 4.3$ in (c), and $p = 6.0$ in (d).

postquench Hamiltonian, we can build the energy distribution and derive the respective moments and cumulants. By following same procedures presented in the method section, we can obtain the Loschmidt zeros.

In Fig. 4, we present the procedure of determination the critical points from 10^6 energy measurements. In this calculation, we limit the summation in Eq. (8) to the range $k = 0$ to $k = 11$. Thus, we can extract the 12 zeros closest to the origin using Loschmidt cumulants of order $n = 4$ to $n = 27$. This predicts the critical time to be around $t U/\hbar = 3.75$ which is the same as the critical time obtained using movable basepoint as in Fig. 2(b). This demonstrates the ability to predict the first DQPT critical time using initial energy fluctuations. The determination of a dynamical Lee-Yang zeros was accomplished in Ref. [37] through the measurement of high cumulants. It should be noted that obtaining precise energy measurements of a many-body quantum system is challenging. Thus, the presented method offers an approach to establish a connection between DQPTs in the Bose-Hubbard model and measurable quantities i.e., energy fluctuations, at least in principle.

VI. CONCLUSION

In summary, we have investigated the Loschmidt zeros associated with the dynamical quantum phase transitions in the Bose-Hubbard model and the extended Bose-Hubbard model. This analysis was conducted through the utilization of the Loschmidt cumulants method. We have determined the locations of zeros of the Loschmidt amplitude in the complex plane of time. And by identifying the crossing point with the imaginary axis we get the dynamical phase transition point to an discrepancy lower than 2% for the Bose-Hubbard model. For the extended Bose-Hubbard model, the first transition point are determined. The discrepancy is lower than 6% for final quench parameters that are distant from the equilibrium critical points.

We use system size of 4 to 10. A modest system size requirement can facilitate the investigation of DQPTs in the Bose-Hubbard model of higher dimensions. Also, we show an avenue for determining the dynamical phase transition by measuring the initial state energy fluctuation in the

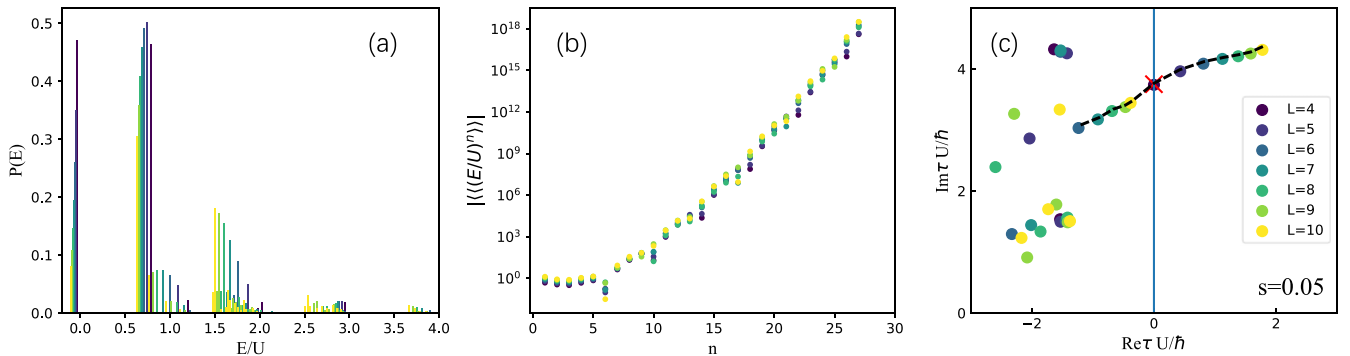


FIG. 4. Determination of the critical time from the initial energy fluctuation. We quench the system from the superfluid phase $s_0 = 0.36$ to the Mott insulator phase $s = 0.05$. (a) The energy distribution obtained from 10^6 energy measurements of the postquench Hamiltonian. (b) Energy cumulants determined from the energy distribution. (c) Determination of the Loschmidt zeros using cumulants of orders $n = 4$ to $n = 27$. The dashed lines are drawn to guide the eyes. The critical point can be identified as the intersection of the line with the imaginary axis.

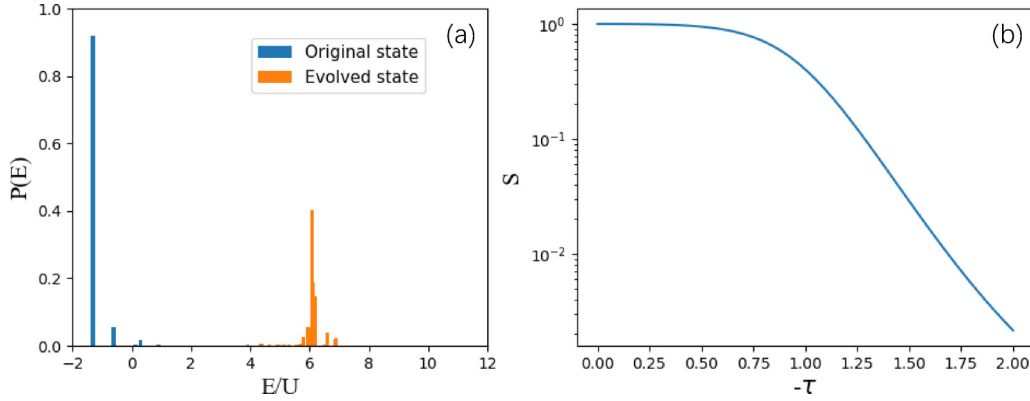


FIG. 5. Energy distribution of the evolved state. (a) The energy distribution of the original state $|\psi_0\rangle$ and the time evolved state $\frac{e^{-\tau\hat{H}}|\psi_0\rangle}{\|e^{-\tau\hat{H}}|\psi_0\rangle\|}$ at $\tau = -2$. (b) Evolution of spectrum overlap S .

Bose-Hubbard model. This may pave way for experimental observation of DQPTs in the Bose-Hubbard model.

ACKNOWLEDGMENTS

This work is supported by the National Natural Science Foundation of China (Grants No. 11920101004, No. 11934002, No. 12174006), and the National Key Research and Development Program of China (Grants No. 2021YFA1400900 and No. 2021YFA0718300).

APPENDIX A: ENERGY DISTRIBUTION OF THE EVOLVED STATE

Given the basic definition of DQPT: $Z(\tau) = \langle \psi_0 | e^{-\tau\hat{H}} | \psi_0 \rangle$, here we compare the energy distribution of $|\psi_0\rangle$ and the normalized wave function $\frac{e^{-\tau\hat{H}}|\psi_0\rangle}{\|e^{-\tau\hat{H}}|\psi_0\rangle\|}$. In the case of Fig. 2(e), $|\psi_0\rangle$ is the ground state of the prequench Hamiltonian. For $\frac{e^{-\tau\hat{H}}|\psi_0\rangle}{\|e^{-\tau\hat{H}}|\psi_0\rangle\|}$, if τ go to the left part of complex plane the real time evolution would enlarge the high energy part of the energy distribution. As a result, $|\psi_0\rangle$ and $\frac{e^{-\tau\hat{H}}|\psi_0\rangle}{\|e^{-\tau\hat{H}}|\psi_0\rangle\|}$ will be orthogonal. We calculate the case in Fig. 2(e) using lengths

of 8. As we see in Fig. 5(a), negligible overlap exists between the energy distribution $P^{(O)}(E)$ and $P^{(E)}(E)$ when $\tau = -2$. In Fig. 5(b), we also show the evolution of the spectrum overlap $S = \sum_i \sqrt{P^{(O)}(E_i)}\sqrt{P^{(E)}(E_i)}$. As τ goes to the negative direction of the real axis, the overlap decreases continuously.

APPENDIX B: CORRELATION FUNCTION AND THE FINITE-SIZE EFFECTS

Here we assess the finite-size effects by analyzing the correlation function. For the case in Figs. 3(b)–3(d), the ground state is the density wave phase. So we consider the density wave correlation function $C_{DW}(r) = (-1)^r \langle \delta n_0 \delta n_r \rangle$ [34], where $\delta n_r = n_r - \bar{n}$ denotes the number fluctuations from average filling. We compute the correlation function associated with Figs. 3(b) and 3(c). The results are shown in Fig. 6. Both the correlation functions approach constants in the long-range limit. While in the short range, they behave differently. The correlation function saturates to a constant quickly in Fig. 6(b). While in Fig. 6(a) the correlation function saturates to a constant around $r = \pm 5$ which is comparable to the length scale we adopted. This may result in more pronounced finite-size effects.

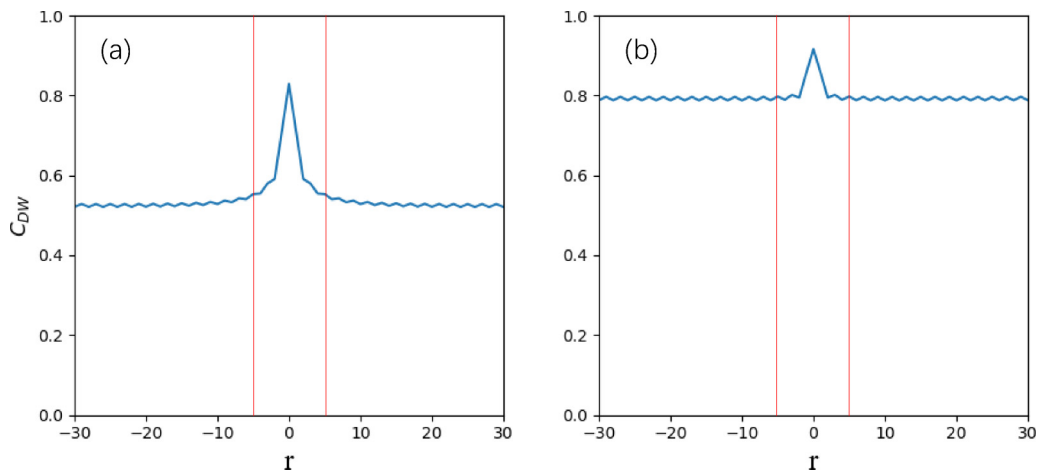


FIG. 6. Correlation functions in the DW phase. The red lines indicate $r = \pm 5$. (a) and (b) are the DW correlation with parameter $p = 3.7$ and $p = 4.3$.

- [1] A. Mitra, *Annu. Rev. Condens. Matter Phys.* **9**, 245 (2018).
- [2] T. Langen, T. Gasenzer, and J. Schmiedmayer, *J. Stat. Mech.* (2016) 064009.
- [3] J. Dziarmaga, *Adv. Phys.* **59**, 1063 (2010).
- [4] S. Will, T. Best, U. Schneider, L. Hackermuller, D. S. Luhmann, and I. Bloch, *Nature (London)* **465**, 197 (2010).
- [5] F. Wilczek, *Phys. Rev. Lett.* **109**, 160401 (2012).
- [6] N. Goldman and J. Dalibard, *Phys. Rev. X* **4**, 031027 (2014).
- [7] J. Eisert, M. Friesdorf, and C. Gogolin, *Nat. Phys.* **11**, 124 (2015).
- [8] T. F. J. Poon and X.-J. Liu, *Phys. Rev. A* **93**, 063420 (2016).
- [9] J. Zhang, G. Pagano, P. W. Hess, A. Kyprianidis, P. Becker, H. Kaplan, A. V. Gorshkov, Z. X. Gong, and C. Monroe, *Nature (London)* **551**, 601 (2017).
- [10] M. Heyl, A. Polkovnikov, and S. Kehrein, *Phys. Rev. Lett.* **110**, 135704 (2013).
- [11] M. Heyl, *Rep. Prog. Phys.* **81**, 054001 (2018).
- [12] U. Bhattacharya, S. Bandyopadhyay, and A. Dutta, *Phys. Rev. B* **96**, 180303(R) (2017).
- [13] S. Sharma, U. Divakaran, A. Polkovnikov, and A. Dutta, *Phys. Rev. B* **93**, 144306 (2016).
- [14] M. Heyl and J. C. Budich, *Phys. Rev. B* **96**, 180304(R) (2017).
- [15] J. C. Budich and M. Heyl, *Phys. Rev. B* **93**, 085416 (2016).
- [16] C. Karrasch and D. Schuricht, *Phys. Rev. B* **95**, 075143 (2017).
- [17] M. Heyl, *Phys. Rev. Lett.* **115**, 140602 (2015).
- [18] S. De Nicola, A. A. Michailidis, and M. Serbyn, *Phys. Rev. Lett.* **126**, 040602 (2021).
- [19] N. Fläschner, D. Vogel, M. Tarnowski, B. S. Rem, D. S. Lühmann, M. Heyl, J. C. Budich, L. Mathey, K. Sengstock, and C. Weitenberg, *Nat. Phys.* **14**, 265 (2018).
- [20] K. Wang, X. Qiu, L. Xiao, X. Zhan, Z. Bian, W. Yi, and P. Xue, *Phys. Rev. Lett.* **122**, 020501 (2019).
- [21] Q. Huang, R. Yao, L. Liang, S. Wang, Q. Zheng, D. Li, W. Xiong, X. Zhou, W. Chen, X. Chen, and J. Hu, *Phys. Rev. Lett.* **127**, 200601 (2021).
- [22] S. Braun, M. Friesdorf, S. S. Hodgman, M. Schreiber, J. P. Ronzheimer, A. Riera, M. del Rey, I. Bloch, J. Eisert, and U. Schneider, *Proc. Natl. Acad. Sci.* **112**, 3641 (2015).
- [23] Q. Zheng, Y. Wang, L. Liang, Q. Huang, S. Wang, W. Xiong, X. Zhou, W. Chen, X. Chen, and J. Hu, *Phys. Rev. Res.* **5**, 013136 (2023).
- [24] M. Lacki and M. Heyl, *Phys. Rev. B* **99**, 121107(R) (2019).
- [25] S. Stumper, M. Thoss, and J. Okamoto, *Phys. Rev. Res.* **4**, 013002 (2022).
- [26] M. Schmitt and S. Kehrein, *Phys. Rev. B* **92**, 075114 (2015).
- [27] S. Vajna and B. Dóra, *Phys. Rev. B* **91**, 155127 (2015).
- [28] S. Peotta, F. Brange, A. Deger, T. Ojanen, and C. Flindt, *Phys. Rev. X* **11**, 041018 (2021).
- [29] F. Brange, S. Peotta, C. Flindt, and T. Ojanen, *Phys. Rev. Res.* **4**, 033032 (2022).
- [30] C. N. Yang and T. D. Lee, *Phys. Rev.* **87**, 404 (1952).
- [31] T. D. Lee and C. N. Yang, *Phys. Rev.* **87**, 410 (1952).
- [32] F. Brange, T. Pyhäranta, E. Heinonen, K. Brandner, and C. Flindt, *Phys. Rev. A* **107**, 033324 (2023).
- [33] G. B. Arfken, H. J. Weber, and F. E. Harris, in *Mathematical Methods for Physicists*, edited by G. B. Arfken, H. J. Weber, and F. E. Harris (Academic Press, Boston, 2013), 7th ed., pp. 469–550.
- [34] D. Rossini and R. Fazio, *New J. Phys.* **14**, 065012 (2012).
- [35] S. Stumper and J. Okamoto, *Phys. Rev. A* **101**, 063626 (2020).
- [36] S. Ejima, F. Lange, and H. Fehske, *Phys. Rev. Lett.* **113**, 020401 (2014).
- [37] K. Brandner, V. F. Maisi, J. P. Pekola, J. P. Garrahan, and C. Flindt, *Phys. Rev. Lett.* **118**, 180601 (2017).